

A novel *SART3::RARG* fusion gene in acute myeloid leukemia with acute promyelocytic leukemia phenotype and differentiation escape to retinoic acid

Acute promyelocytic leukemia (APL) is a unique subtype of acute myeloid leukemia (AML) that features promyelocytic leukemia cells, prominent coagulopathy, and the promyelocytic leukemia (*PML*::retinoic acid receptor α (*RARA*)) fusion gene derived from translocation t(15;17).¹ The introduction of all-trans retinoic acid (ATRA) and later arsenic trioxide (ATO) has revolutionized the treatment of this disease, which is now highly curable.¹ In approximately 5% of the cases presenting APL phenotype, *PML::RARA* was negative. By far, translocations involving *RARA* and 16 other partner genes have been reported with different sensitivity to ATRA.² Rearrangement involving the other two members of the retinoic acid receptor family, retinoic acid receptor β (*RARB*) or retinoic acid receptor γ (*RARG*), has been reported including *TBLR1::RARB*, *NUP98::RARG*, *CPSF6::RARG*, *PML::RARG*, *NPM1::RARG::NPM1*, *HNRNPC::RARG* and *RARG::HNRNPM*.²⁻⁵ All of these patients demonstrated ATRA resistance. Here, we report a novel *SART3::RARG* fusion gene in a case of APL-like leukemia (APLL) showing differentiation escape to ATRA. A comprehensive analysis of the patient and preliminary function assays for *SART3::RARG* were performed. Our work not only enriches our knowledge of APL-like leukemia (APLL), but also lends support to the proposal that *RARG* rearrangement represent a distinct subtype of AML that needs early recognition and proper management.

A 46-year-old previously healthy man was admitted because of gum bleeding and spontaneous ecchymosis. His initial complete blood count showed a white blood cell (WBC) count of $2.0 \times 10^9/L$, hemoglobin level of 99 g/L, and platelet count of $80 \times 10^9/L$. Prominent coagulopathy was noted with prothrombin time of 20.1 seconds (s) (reference 10–14 s), activated partial thromboplastin time of 60.6 s (reference 28–45 s), fibrinogen level of 0.33 g/L (reference 2–4 g/L), fibrinogen/fibrin degradation product levels 27.67 mg/L (reference, 0–5 mg/L), and D-dimer levels 4.37 mg/L (reference, 0–0.5 mg/L). Bone marrow (BM) smear showed hypercellularity with 81.7% abnormal promyelocytes (Figure 1A). The blasts featured abundant cytoplasmic coarse granules, lobulated or kidney-shaped nuclear, and occasional nucleoli, reminiscent of APL. Auer rods were absent. Myeloperoxidase (MPO) staining was negative somehow (Figure 1B). These cells were positive for CD13, CD33, and CD117, partially positive for MPO, CD64, and CD15, but negative for CD34, HLA-DR, CD11b, CD14, and other lymphoid-related markers by flow cytometry (Figure 1E). Flu-

orescence *in situ* hybridization (FISH) using a *PML::RARA* dual-color dual-fusion probe showed no fusion signals (Figure 1C). Multiplex reverse transcription polymerase chain reaction (RT-PCR) detecting 43 leukemia-related fusion genes including *PML::RARA* were negative. G-banding karyotype analysis of BM cells revealed a clonal -Y in 16 of 20 metaphase analyzed (Figure 1C). ATRA (20 mg, twice daily) was administered on suspicion of APL for a week without improvement of coagulopathy. He was transferred to our hospital on the 8th day. We continued ATRA treatment and reevaluated his BM morphology and immunophenotype, where there were no signs of differentiation. Meanwhile, his WBC count increased to $6.4 \times 10^9/L$, and he complained of bone pain. Despite strong transfusion supportive care, he died of diffuse alveolar hemorrhage on the 11th day.

Given the absence of *PML::RARA*, RNA sequencing, single-nucleotide polymorphism (SNP) array, and whole exome sequencing (WES) were performed using the patient's BM sample to characterize underlying molecular aberrations. The study was approved by the Second Xiangya Hospital Institutional Review Board, Central South University. Informed consent or assent was obtained in accordance with the Declaration of Helsinki. RNA sequencing revealed that *SART3* exon 18 was fused to *RARG* exon 3 (Figures 2A). In order to validate this novel fusion, RT-PCR was performed with the forward primer 5'-TCAAAGTGGCAATCAGCAACC-3' (at *SART3* exon 18), and reverse primer 5'-AGCCTGGGAGGCTCCGTA-3' (at *RARG* exon 3). An expected 160 bp band was visualized on agarose gel electrophoresis (Figure 2B) (GenBank accession number ON681589). Using the same primers, a 1,156 bp transcript was amplified from the genomic DNA of BM sample, which localized the genomic breakpoint at *SART3* intron 18 (Chr12: 108917694) and *RARG* intron 2 (Chr12: 53622069) (Figure 2C) (GenBank accession number ON681590). The reciprocal *RARG::SART3* fusion was not detected. The fusion was in-frame and encode a 1,406-amino acid chimera (Figure 2E). Immunoblotting of BM mononuclear cell lysate using an anti-*RARG* antibody (Cell Signaling Technology) confirmed the presence of *SART3::RARG* as a band (~170 kDa) was visualized in addition to the wild-type *RARG* band (~55 kDa) (Figure 2D).

Furthermore, SNP array revealed a mosaic loss of chromosome Y in accordance with karyotype (*Online Supplementary Figure S1A*). Besides, a 2.26 Mb microdeletion in

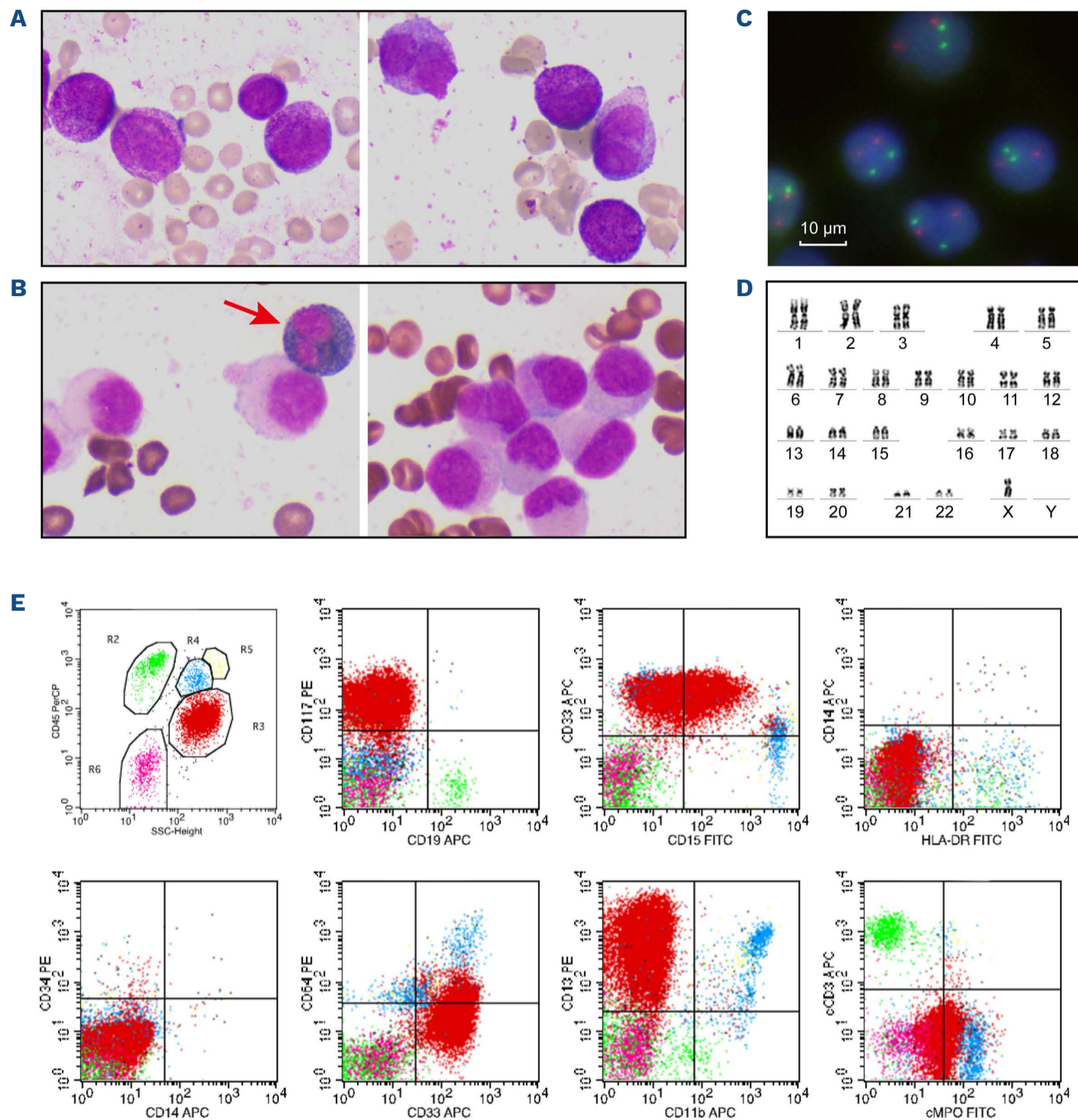


Figure 1. Morphologic, immunophenotypic, and cytogenetic features of the *SART3::RARG*-positive blasts. (A) Wright-Giemsa staining of bone marrow smear showing hypergranular promyelocytes without Auer rods. Original magnification X1,000. (B) Cytochemical evidence for myeloperoxidase negativity of blast cells (as compared with neutrophils; arrows). Original magnification X1,000. (C) Interphase fluorescence *in situ* hybridization using the *PML::RARA* dual-color, dual-fusion translocation probe revealed the absence of *PML::RARA*. (D) Karyotypic analysis of the bone marrow revealed a karyotype of 45,X,-Y[16]/46,XY[4]. (E) Immunophenotype of the patient with *SART3::RARG*-positive AML. Dot plots of flow cytometry data of bone marrow aspiration sample. Red cluster shows the blast population.

12q21.2, a 1.99 Mb microdeletion in 12q23.3q24.11 encompassing *SART3* (Online Supplementary Figure S1B), and a uniparental disomy of a 5.42 Mb segment at 17q21.2q21.32 (Online Supplementary Figure S1C) were detected. Since *SART3* and *RARG* located at 12q23.3 and 12q13.13, respectively, the *SART3::RARG* fusion gene may result from the microdeletions or cryptic translocations in 12q. In addition, WES identified two somatic mutations, *WT1* c.1114-2A>G (variant allele frequency [VAF] 27%) (Online Supplementary Figure S2A) and *KDM6A*

p.Pro1107AlafsTer46 (VAF 90.5%) (Online Supplementary Figure S2B), which were verified by RT-PCR and Sanger sequencing. Moreover, three *MPO* mutations (Online Supplementary Table S1) were detected by WES, which might have impaired the enzymatic and immunological activity of *MPO* in a way of compound heterozygous mutations, leading to negative *MPO* staining and reduced *MPO* immunophenotype in this case.⁶

Retinoic acid receptors (RAR) are members of nuclear hormone receptors, and regulate cell growth, differentiation,

and cell death in response to retinoic acid/ligand binding. Their modular structure features two main functional domains: DNA-binding domain (DBD) and ligand-binding domain (LBD). The three RAR family members, RARA, RARB, and RARG, share high sequence homology but show distinct transcriptional properties.⁷ During hematopoiesis, RARG is a potent ligand-dependent transactivator that governs hemopoietic stem/progenitor cells self-renewal,

whereas RARA exerts ATRA-reversible basal repressive functions favoring myeloid differentiation.⁷ SART3 (spliceosome-associated factor 3, U4/U6 recycling protein), is a nuclear RNA-binding protein regulates pre-mRNA splicing, translesion DNA synthesis, and histone chaperoning.^{8,9} It plays important roles in viral and host gene transcription, embryonic development, and hematopoiesis.⁸⁻¹⁰ Structurally, SART3 consist of multiple half-a-

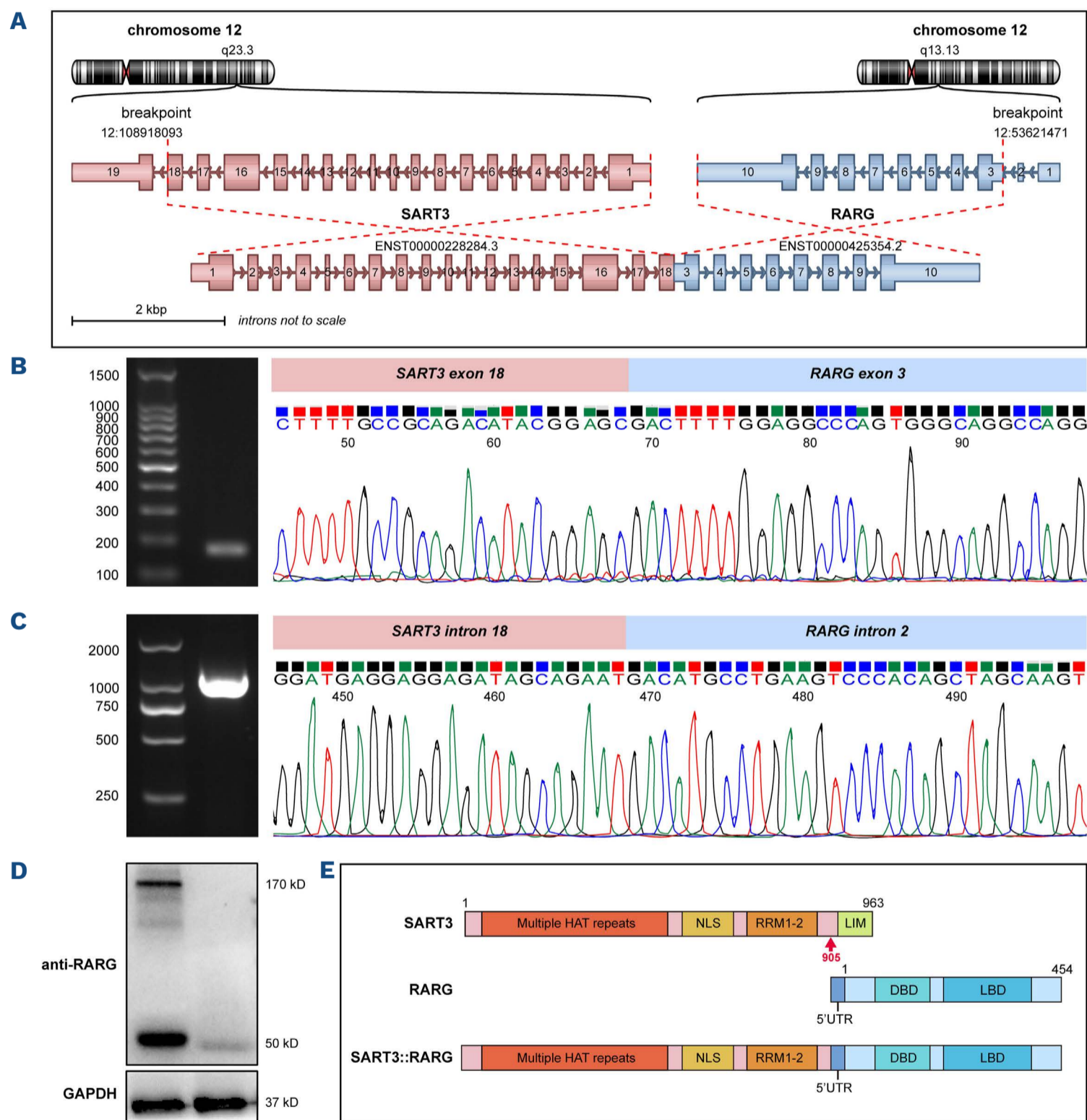


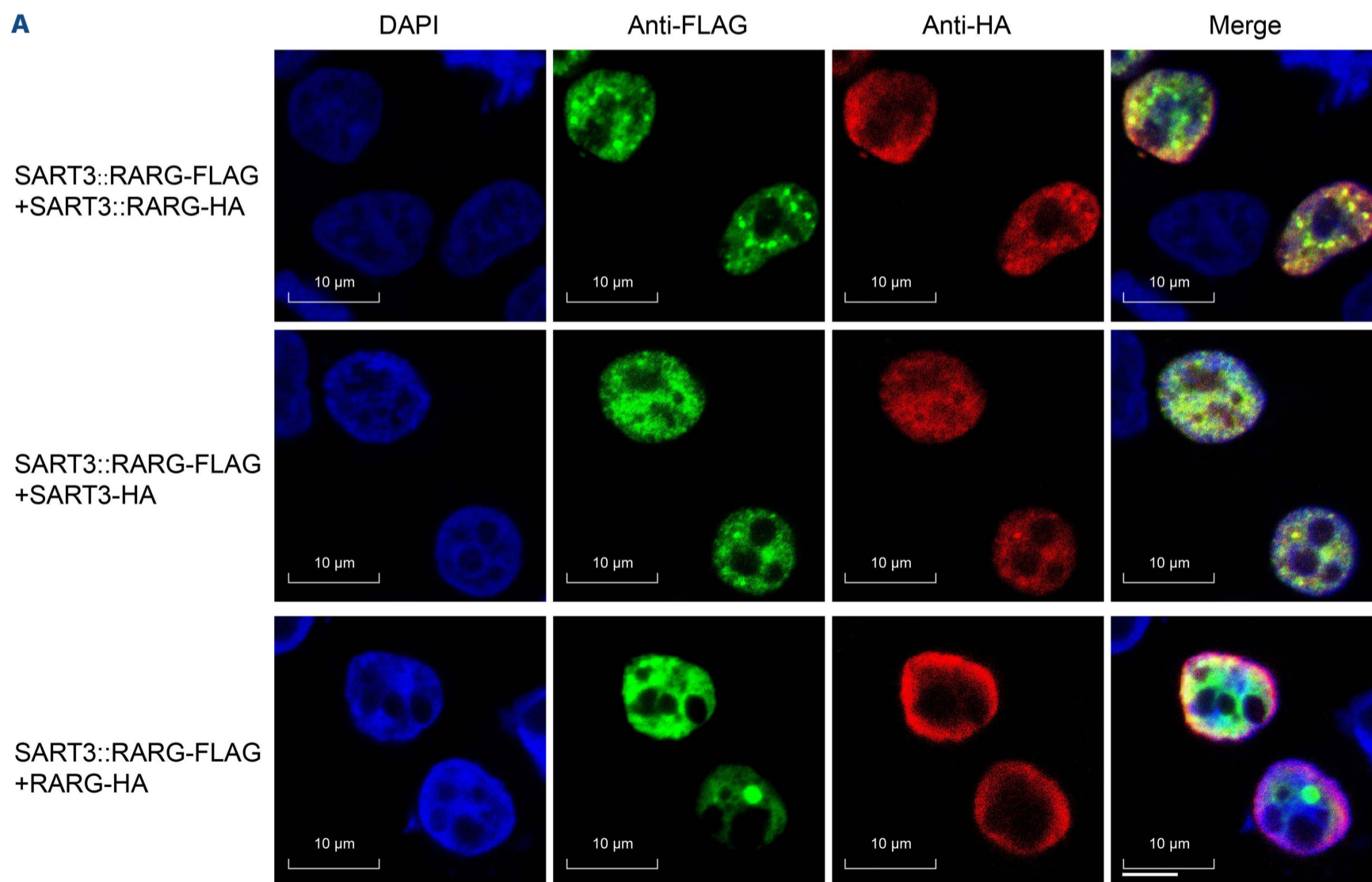
Figure 2. Molecular characterization of the *SART3::RARG* fusion. (A) RNA sequencing analysis revealed the fusion between exon 18 of *SART3* and exon 3 of *RARG*. (B) Reverse transcription polymerase chain reaction (RT-PCR) using bone marrow (BM) cDNA confirmed the *SART3::RARG* fusion transcript when a 160 bp band was visualized. Partial nucleotide sequences surrounding the junction was shown. (C) RT-PCR for *SART3::RARG* using BM genomic DNA amplified a band of 1,156 bp. Partial nucleotide sequences surrounding the genomic breakpoint was shown. (D) Western blotting of BM mononuclear cell lysate using anti-RARG antibody showed two bands corresponding to the wild-type RARG (~55 kDa) and the *SART3::RARG* chimera (~170 kDa) in the patient. 1: the patient with *SART3::RARG*; 2: a classic APL patient with *PML::RARA*. (E) Schematic diagram of *SART3*, *RARG*, and the *SART3::RARG* fusion protein. The fusion breakpoint was highlighted with a red arrow. DBD: DNA binding domain; HAT: half-a-tetratricopeptide repeats; LBD: ligand binding domain; LIM: LSM-interacting motif; NLS: nuclear localization sequence; RRM1-2: RNA recognition motifs 1-2; 5' UTR: 5' untranslated region.

tetratricopeptide (HAT) repeats, a nuclear localization signal (NLS) sequence, two RNA recognition motifs (RRM), and a LSM-interaction motif (LIM) at the C-terminus (Figure 2E). *SART3::PDGFRB* was reported in a patient with eosinophilia-associated myeloproliferative neoplasm.¹¹ The *SART3::RARG* chimera retained the HAT repeats, NLS, and RRM of *SART3*, an intact *RARG*, and additional 46 amino acids due to inclusion of partial *RARG* 5' untranslated region (UTR) (Figure 2E). The loss of 58 amino acids in the carboxyl terminal of *SART3*, including the LIM domain, may impair *SART3*'s function as an mRNA splicing regulator.

As shown by immunofluorescence experiments, the subcellular localization of *SART3::RARG* was primarily intranuclear, diffusely distributed and specifically aggregated in large bright dots (Figure 3A, the second column) similar to that of *SART3*¹² but distinct from *RARG*. Homo-dimerization is a common feature of *RARA* fusion chimeras as well as *NUP98::RARG* to gain oncogenic potential.¹³ As shown in Figure 3A, FLAG-tagged *SART3::RARG* co-localized with either HA-tagged *SART3::RARG* or *SART3*, but not *RARG*. Co-immunoprecipitation results confirmed the self-association of *SART3::RARG* and its heterodimerization with *SART3*, but not with *RARG* (Figure 3B), suggest that homodimerization of *SART3::RARG* is mediated by the *SART3* portion, likely the HAT repeats.⁹ Furthermore, dual

luciferase reporter assays revealed that *SART3::RARG* acts as a dominant-negative *RARG* mutant (Figure 3C) similar to *NUP98::RARG*¹³. In response to ATRA, the transcriptional activity of *RARA*, *PML::RARA*, and *RARG* increased dramatically whereas *SART3::RARG* showed a blunt ATRA response comparable to ATRA-insensitive *ZBTB16::RARA* and *GTF2I::RARA*¹⁴ (Figure 3D).

Including *SART3::RARG*, seven different *RARG* fusion genes have been reported.²⁻⁵ Although the breakpoint in *RARG* varied, occurring at exon 1, 2, 3, or 4 for *X::RARG* and at intron 9 for *RARG::X*, all these *RARG* fusion chimeras retain the DBD and LBD of *RARG*. From cases reported in the literature, these *RARG*-rearranged AML were predominantly East Asians, and exhibited APL morphology and immunophenotype, bleeding diathesis, but were insensitive to ATRA. Response to anthracycline plus cytarabine "7+3" induction regimen varied, while incorporating homoharringtonine into reinduction chemotherapy succeed in achieving complete remission. Due to its rarity, the incidence and prognosis of *RARG*-rearranged AML remain to be determined. The early death of our patient makes it hard to conclude clinical ATRA resistance. However, the lack of an early response suggests ATRA insensitivity. It is reported that CD11b positivity and correction of coagulation disorders are early signs of ATRA's efficacy.¹⁵ In our



Continued on following page.

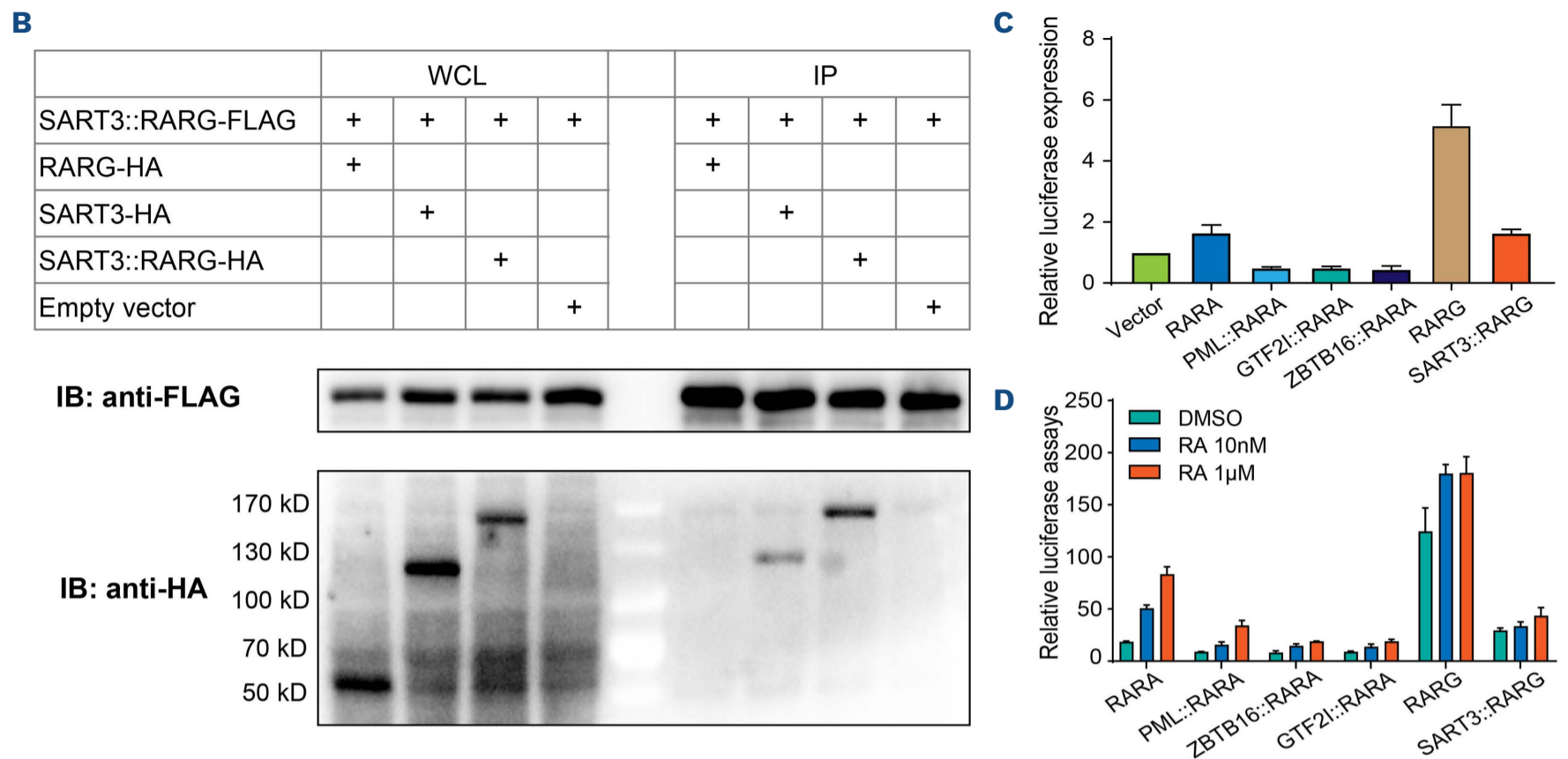


Figure 3. Functional assays for the *SART3::RARG* fusion chimera. (A) Subcellular localization/colocalization of *SART3::RARG*, *SART3*, and *RARG*. 293T cells were co-transfected with indicated pcDNA3.1 expression plasmids. Immunofluorescence was performed with anti-FLAG and anti-HA antibodies. The nuclei were visualized with 4', 6-diamidino-2-phenylindole (DAPI: blue, the first column), FLAG-tagged *SART3::RARG* was stained with Alexa Fluor 488 (green, the second column), and HA-tagged proteins were stained with Alexa Fluor 594 (red, the third column). The 4th column shows composite images: yellow fluorescence indicates co-localization. Original magnification X630. (B) *SART3::RARG* interacts with itself or *SART3*, but not *RARG*. PcDNA3.1 expression plasmids of *SART3::RARG*-FLAG was co-transfected into 293T cells with either empty vector or HA-tagged expression vector, as shown in the table. Immunoblotting of whole cell lysate (WCL) confirmed successful transfection and expression (left). Cell lysate were immunoprecipitated (IP) using anti-FLAG antibodies, and analyzed by immunoblotting (right). *SART3::RARG*-HA and *SART3*-HA, but not *RARG*-HA, could be detected after immunoprecipitation with anti-FLAG antibodies. (C) *SART3::RARG* act as a negative mutant of *RARG*. 293T cells were transfected with 4×*RARE* pGL3 reporter vector, pRL-TK, and together with a vector containing one of the following genes: *RARA*, *PML::RARA*, *GTF2I::RARA*, *ZBTB16::RARA*, *RARG*, or *SART3::RARG*. Relative firefly luciferase expression of cell lysate was normalized to Renilla luciferase. The expression of the vector control was set to 1. The error bars represent the mean of an experiment performed in triplicate. (D) *SART3::RARG* responds poorly to ATRA. 293T cells transfected with the indicated constructs were treated with dimethyl sulfoxide (DMSO), 10 nm ATRA, or 1 µM ATRA for 48 hours. Relative firefly luciferase expression of cell lysate was normalized to Renilla luciferase. N=3 independent experiments. All data are presented as mean ± standard deviation.

patient, 7 days' of ATRA therapy failed to upregulate CD11b expression, which were seen as a sign of granulocytic differentiation,¹⁵ suggested differentiation escape to ATRA. A total of 10 days' ATRA treatment together with strong transfusion-supported care, did not bring improvement of coagulopathy, suggested ATRA ineffectiveness. Given the observation that other *RARG*-rearranged patients were insensitive to ATRA, we propose ATRA withdraw and switching to AML-like approaches in *RARG*-rearranged APL. Early identification and strong transfusion supportive care are crucial to avoid early death, whereas optimal treatment requires further investigation.

In summary, we have identified a novel *SART3::RARG* fusion gene in a patient with APL phenotype. Our finding enriched the understanding of APL. Further studies are needed to elucidate the critical role of *SART3::RARG* and *RARG* dysregulation in leukemogenesis and for guiding treatment approaches.

Authors

Ji Li,¹ Yang Zhang,² Junjun Li,³ Yunxiao Xu¹ and Guangsen Zhang¹

¹Department of Hematology, the Second Xiangya Hospital of Central South University, Changsha; ²Department of Oncology, the Second Xiangya Hospital of Central South University, Changsha and

³Department of Hematology, the First Affiliated Hospital of University of South China, Hengyang, Hunan, China

Correspondence:

G. ZHANG - zgslly@163.com

<https://doi.org/10.3324/haematol.2022.281766>

Received: July 21, 2022.

Accepted: October 11, 2022.

Prepublished: October 27, 2022.

©2023 Ferrata Storti Foundation

Published under a CC BY-NC license 

Disclosures

No conflicts of interest to disclose.

Contributions

JL and GZ designed the study, performed the study, and wrote the manuscript. YZ, JL and YX collected data, and interpreted the data.

Acknowledgements

The authors thank the patients and their family for their

contribution to this study. We thank Xiaojiao Sun and Weihong Yang from Kindstar Diagnostics (Wuhan, Hubei, China) for performing next-generation sequencing and assisting with bioinformatics.

Funding

This work was supported by grants from the National Natural Science Foundation of China (grant no. 81700168 to JL) and (grant no. 81500171 to YZ), and Natural Science Foundation of Hunan Province (grant no. 2019JJ40449 to YZ).

Data-sharing statement

Questions regarding data sharing should be addressed to the corresponding author. For original data, please contact zgslly@163.com, or lijiji26@163.com.

References

1. Sanz MA, Fenaux P, Tallman MS, et al. Management of acute promyelocytic leukemia: updated recommendations from an expert panel of the European LeukemiaNet. *Blood*. 2019;133(15):1630-1643.
2. Geoffroy MC, de The H. Classic and variants APLs, as viewed from a therapy response. *Blood*. 2019;133(15):1630-1643.
3. Song Y, Hou J, Wan L, et al. A short report of novel RARG-HNRNPM fusion gene in resembling acute promyelocytic leukemia. *Hematology*. 2022;27(1):518-522.
4. Chen X, Wang F, Zhang Y, et al. A novel NPM1-RARG-NPM1 chimeric fusion in acute myeloid leukaemia resembling acute promyelocytic leukaemia but resistant to all-trans retinoic acid and arsenic trioxide. *Br J Cancer*. 2019;120(11):1023-1025.
5. Su Z, Liu X, Xu Y, et al. Novel reciprocal fusion genes involving HNRNPC and RARG in acute promyelocytic leukemia lacking RARA rearrangement. *Haematologica*. 2020;105(7):e376-e378.
6. Heiblig M, Paubelle E, Plesa A, et al. Comprehensive analysis of a myeloperoxidase-negative acute promyelocytic leukemia. *Blood*. 2017;129(1):128-131.
7. Geoffroy MC, Esnault C, de The H. Retinoids in hematology: a timely revival? *Blood*. 2021;137(18):2429-2437.
8. Huang M, Zhou B, Gong J, et al. RNA-splicing factor SART3 regulates translesion DNA synthesis. *Nucleic Acids Res*. 2018;46(9):4560-4574.
9. Whitmill A, Timani KA, Liu Y, He JJ. Tip110: physical properties, primary structure, and biological functions. *Life Sci*. 2016;149:79-95.
10. Liu Y, Timani K, Mantel C, et al. TIP110/p110nrb/SART3/p110 regulation of hematopoiesis through CMYC. *Blood*. 2011;117(21):5643-5651.
11. Erben P, Gosenca D, Muller MC, et al. Screening for diverse PDGFRA or PDGFRB fusion genes is facilitated by generic quantitative reverse transcriptase polymerase chain reaction analysis. *Haematologica*. 2010;95(5):738-744.
12. Van Nostrand EL, Freese P, Pratt GA, et al. A large-scale binding and functional map of human RNA-binding proteins. *Nature*. 2020;583(7818):711-719.
13. Qiu JJ, Zeisig BB, Li S, et al. Critical role of retinoid/rexinoid signaling in mediating transformation and therapeutic response of NUP98-RARG leukemia. *Leukemia*. 2015;29(5):1153-1162.
14. Li J, Zhong HY, Zhang Y, et al. GTF2I-RARA is a novel fusion transcript in a t(7;17) variant of acute promyelocytic leukaemia with clinical resistance to retinoic acid. *Br J Haematol*. 2015;168(6):904-908.
15. Horna P, Zhang L, Sotomayor EM, Lancet JE, Moscinski LC. Diagnostic immunophenotype of acute promyelocytic leukemia before and early during therapy with all-trans retinoic acid. *Am J Clin Pathol*. 2014;142(4):546-552.